Supplementary materials for the manuscript: Interactions between serotypes of dengue highlight epidemiological impact of cross-immunity

Nicholas G. Reich, Sourya Shrestha, Aaron A. King, Pejman Rohani,
Justin Lessler, Siripen Kalayanarooj, In-Kyu Yoon, Robert V. Gibbons,
Donald S. Burke, Derek A. T. Cummings

May 29, 2013

1 Methodological details for multi-pathogen TSIR model

1.1 Introduction to the TSIR model

The time series susceptible infected recovered (TSIR) model, developed by Finkenstädt and Grenfell [2000], has proven to be an effective tool for drawing inferences about parameters that govern dynamic infectious disease systems (see, for example, Ferrari et al. [2008], Metcalf et al. [2009], Finkenstädt and Grenfell [2002]). The TSIR model serves as a bridge between simple auto-regressive time-series models (where a case count at time t is modeled as a function of a previous observation, say from time $t-1$) and more complex individual-level mechanistic transmission models for infectious disease. The machinery of the TSIR model monitors the changing patterns over time of the fraction of a population susceptible to a particular pathogen. In this way, more subtle patterns in observed data may be explained, such as the biannual cycles of measles epidemics captured by Finkenstädt and Grenfell in their original TSIR paper.

Our aim has been to extend this single-pathogen TSIR framework to account for the more complex interactions between multiple pathogens. To this end, we developed a discrete-time stochastic epidemic model for a multi-serotype disease, such as dengue fever. To model the between-pathogen interactions, we assume that infection with one serotype of dengue confers permanent immunity from reinfection with the same serotype and temporary protection against infection with other serotypes. Overall, there are four serotypes of dengue.

1.2 The core components of the TSIR model

The TSIR model is fit in a two-stage process. First, an algorithm performs the susceptible accounting for the model based on the observed data. Essentially, this step computes the variation in the susceptible fraction over time. Second, the results from the susceptible accounting are incorporated into a log-linear transmission model that is fit to the data.

Susceptible accounting

The compartment model representing the possible trajectories of individuals through the state-space for a particular serotype is represented in Supplemental Figure 6. State CP represents a convalescent or cross-protected state in which an individual is temporarily recovering from an infection with another serotype and is not susceptible to infection with the serotype in question.

To reconstruct the susceptible dynamics, the original TSIR model used a model of the form

$$S_t = B_{t-d} + S_{t-1} - I_t \tag{1}$$

where I_t and S_t represent, respectively, the counts of infecteds and susceptibles at time t. B_{t-d} is the number of births entering the susceptible population at time t after a period (of duration d) of maternal antibody protection. For a single-pathogen system, this accounting permanently removes infected individuals from the susceptible pool.

To adapt this model to a multi-pathogen setting with non-permanent immunity, we needed to add a few features to this model for susceptible accounting. First, susceptibility for each serotype needs to be tracked separately. Second, we needed a mechanism to keep track of individuals who were being temporarily removed from the susceptible pool for one serotype due to infection with another serotype. The following equation makes those two adjustments

$$S_{t,i} = B_{t-d} + S_{t-1,i} - I_{t,i} - \delta \cdot Q_{t,-i} \tag{2}$$

where the i subscript denotes serotype i and the $Q_{t,-i}$ terms account for the transitions between susceptible and convalescent states for a particular serotype i. The form of this "Q-term" varies depending on the parametric form assumed for cross-protection, as described below in Sections 1.3 and 1.4. The parameter δ represents the fraction of the infected population which experiences a period of cross-protection. In our primary model, we considered values of δ between 0 and 1. However allowing δ to assume negative values admits another interpretation, namely that δ could describe the relative contribution of those individuals infected with one serotype to a population's susceptibility to a different serotype. In this scenario, negative values of δ are consistent with immune enhancement of severity of or susceptibility to infections among those previously infected.

We assume that the true number of cases is related to the observed number of cases as $I_t = \rho_t C_t$, where C_t is equal to the observed case counts and ρ_t is the inverse of the probability a case is reported at time t. Finkenstädt and Grenfell showed that the deviations from the mean number of susceptibles can be estimated simultaneously with the ρ_t using linear splines or localized linear regression. Similar to equation (11) in Finkenstädt and Grenfell [2000], the form of this model is:

$$Y_t = int_{t,i} + \rho_{t,i} X_{t,i} + \delta Q_{t,-i} + resid_{t,i} \tag{3}$$

where

$$\begin{aligned} Y_t &= \sum_{t'=1}^{t} B_{t'-d} \\ X_{t,i} &= \sum_{t'=1}^{t} C_{t'} \\ Q_{t,-i} &= \sum_{j \neq i} Q_{t,j} \end{aligned}$$

and the $Q_{t,j}$ terms are defined specifically for each parametric representation of the cross-protection model (see Sections 1.3 and 1.4 below). The residuals from these linear models are taken to be the deviations from the mean number of susceptibles and are called $Z_{t,i}$. In practice, we fixed the duration of maternal antibody protection, d, to be 16 weeks.

Equation 3 was fit with cubic splines using the `smooth.spline()` function in R with 3 degrees of freedom. The ρ_t were estimated using the `predict.smooth.spline(..., deriv=1)` function. We chose three degrees of freedom for these fits, assuming one degree of freedom was needed for each decade of data, and also corresponding to the three different time periods of different possible detection rates based on changing laboratory methods [Nisalak et al., 2003]. Fitting splines allowed us to balance the desire to not over-smooth the data and thereby removing dynamics of the susceptible population, with wanting to capture long-term variation (likely increases) in reporting of cases over time. We analyzed the sensitivity of our results to our assumptions about the reporting rates. We fitted models with 2, 3, 4, and 5 degrees of freedom (d.f.) in the cubic spline that estimates the reporting rates. We also fit a model that estimated a constant reporting rate for each serotype. We observed that models with greater than 3 d.f. for the reporting rates overfit the data. This overfitting was made evident by several pronounced cycles of increases and decreases in estimated reporting rates, showing that the spline fits were influenced by serotype-specific outbreaks instead of capturing the longer-term secular trends in reporting. Furthermore, based on AIC and likelihood ratio tests, the model with 3 d.f. outperformed models with fewer degrees of freedom. The central result of this work, that the data support the existence of cross-protection between serotypes of dengue on the order of one to three years, is supported across the entire range of modeling assumptions about the reporting rates that we explored.

However, when trying to fit model 3 a complication arises because the Q-terms (which are used as an offset when fitting equation 3) and the $\rho_{t,i}C_{t,i}$ terms both depend on the reporting fractions, $\rho_{t,i}$. We developed an iterative algorithm to fit the $\rho_{t,i}$ for fixed values of the parameters that govern the dynamics of cross-protection. The algorithm follows these steps:

1. For fixed duration models, fix values of k and δ. For exponential models, fix a value for λ and $\delta = 1$.

2. Assume that we have observations at times $t = 1, ..., T$. Assume that L observations are needed to initialize the system. Then data from $t = 1, ..., L$ are used as initial values and data from

$t = L+1, ..., T$ are used to fit the following models.

3. For each serotype, fit equation 3 letting $Q_{t,-i} = 0$ for $t = L+1, ..., T$ and all i to obtain starting estimates of $\rho_{t,i}$ for $t = L+1, ..., T$. And set $\rho_{t,i} \equiv \hat{\rho}_{1,i}$ for $t = 1, ..., L$
4. Use these initial values of ρ to calculate $Q_{t,-i}$ for $t = L+1, ..., T$ and all i.
5. Using $\delta \cdot Q_{t,-i}$ as an offset, fit equation 3 again, obtaining new values of ρ.
6. Iterate steps 4 and 5 until the $\hat{\rho}$ converge or until a maximum number of iterations is reached.
7. If convergence is achieved, return the $\hat{\rho}_{t,i}$ and $Z_{t,i}$.

The outputs from this algorithm can then be used to fit the transmission model.

Fitting the transmission model

The theoretical transmission model is

$$I_{t,i} = r_t \cdot I_{t-1,i}^{\alpha_1} \cdot S_{t-1,i}^{\alpha_2} \cdot \epsilon_{t,i} \tag{4}$$

where the r_t are a time-varying transmission parameters. The α are mixing parameters, which, if both equal 1, define a population with homogeneous mixing whereas values not equal to 1 have been used to describe departures from mass-action mixing [Liu et al., 1987] and to account for discretization of continuous time transmission processes [Glass et al., 2003]. It is assumed that the error term $\epsilon_{t,i}$ is log-normally distributed and has the following properties: $\mathbb{E}[\log \epsilon_{t,i}] = 0$ and $Var(\log \epsilon_{t,i}) = \sigma_\epsilon^2$.

Using a Taylor series expansion of $\log S_t$ around $\bar{S}$, Finkenstädt and Grenfell show that the following model may be used in place of equation 4

$$\log I_{t,i} = \log r_t^* + \alpha_1 \log I_{t-1,i} + \zeta Z_{t-1,i} + \log \epsilon_{t,i} \tag{5}$$

where $r_t^* = r_t \cdot \bar{S}^{\alpha_2}$ and $\zeta = \alpha_2 / \bar{S}$. We may also reduce the degrees of freedom needed to fit this model by fixing the r_t^* to have period of one year. In the case of fitting bi-weekly data, we use $r_{t \bmod 26}^*$. To fit the model in equation 5 we can replace $I_{t,i}$ by $\hat{\rho}_{t,i} \cdot C_{t,i}$, using the estimated reporting rates from the susceptible accounting. The $Z_{t,i}$ are taken as the residuals from the local linear fits described in the previous section. This model can then be fit as a standard linear regression model and estimated with least squares.

We generated profile likelihood surfaces by iterating through possible parameter combinations and for each parameter set, running both the susceptible accounting and the transmission model. For fixed duration models, this meant sweeping across a two-dimensional grid of $0 \leq \delta \leq 1$ and $0 \leq k \leq 100$ biweeks (3.8 years). Fixed duration models experienced some problems with convergence for some of the large values of k included in the analysis. For this reason, the range of k was truncated to be 100 biweeks, which included the 90% and 95% confidence regions for k and δ. For exponential models, we fixed $\delta = 1$ and let λ vary from 0 to 195 biweeks (7.5 years). When the above process is repeated

for different parameter values, a profile likelihood surface can be created and plotted [Bolker, 2011]. Chi-square tests can be used to determine confidence regions for the parameter(s) of interest.

1.3 Fixed duration model details

Let δ be a parameter indicating the population-average contribution from individuals infected with one serotype to the pool of individuals susceptible to other serotypes. Further, let k represent the fixed duration of cross-protection, for those who experience it. For values of δ between 0 and 1, the model can be explained as everyone in our population experiencing cross-protection in one of two ways: (1) with probability $1-\delta$, an individual experiences no cross-protection, or (2) with probability δ an individual experiences cross-protection of exactly k time units. However allowing δ to assume negative values admits another interpretation, namely that δ could describe the relative contribution of those individuals infected with one serotype to a population's susceptibility to a different serotype. In this scenario, negative values of δ are consistent with immune enhancement of severity of or susceptibility to infections among those previously infected.

To reconstruct the susceptible dynamics, we use a process similar to that of Finkenstadt and Grenfell which is adapted to account for the cross-protection term. We assume that those infected with strain j are removed for k time units from the susceptible class for strain i, where $j \neq i$. Assuming that the first k values of the multi-strain time series are known, we can iterate the formulae to obtain the number of susceptibles at time t for strain i:

$$S_{t,i} = S_{t-1,i} + B_{t-d} - I_{t,i} - \delta \sum_{j \neq i} [I_{t-1,j} - I_{t-(k+1),j}]. \tag{6}$$

This formulation assumes that individuals who have been infected in the past k time-periods with any of the strains do not contribute to the susceptible fraction in the same way that others do. The parameter δ (when defined to lie between 0 and 1) is the fraction of infected individuals that gain transient immunity to all other serotypes for a fixed duration of time, k. These individuals are "removed" from the susceptible population. At each time t, we are removing from the susceptible pool those who have just been infected with any strain and adding back in those who were infected k time units ago, who are now assumed to be leaving the period of cross-protection. We define

$$Q_{t,j} \quad = \quad \sum_{t'=1}^{t} \left[\hat{\rho}_{t'-1,j} C_{t'-1,j} - \hat{\rho}_{t'-(k+1),j} C_{t'-(k+1),j} \right]$$

for all $t > L$.

1.4 Exponential model details

In the exponential framework, we assume that all individuals experience a duration of cross-protection, i.e. δ=1. Additionally, we let T be a random variable that represents an individual's duration of cross-protection, and we assume that T follows an exponential distribution with mean λ. One disadvantage

to using a parametric model that supports arbitrarily large durations of cross-protection (such as the exponential distribution, albeit with small probabilities) is that to fit the TSIR model, the initial conditions of the model need to be fixed. In order to fix the initial susceptible state of our population, we assumed that T followed an exponential distribution that was truncated at time L, meaning no individual remained cross-protected for longer than L time units. In practice, we fixed L at 10 years and 5 months. This length was decided upon because it was the 75th percentile of the exponential distribution with a mean of 7.5 years – *a priori* the highest λ considered.

Given this distribution for the duration of cross-protection, the probability an individual becomes susceptible between $u-1$ and u time units after infection, given that cross-protection will not last more than L time units where $u < L$, is

$$Pr(u-1 < T < u | T < L) = \frac{Pr(u-1 < T < u, T < L)}{Pr(T < L)} = \frac{Pr(u-1 < T < u)}{Pr(T < L)} = \frac{e^{-u/\lambda}(e^{1/\lambda}-1)}{1-e^{-L/\lambda}}.$$

Assuming that the first L values of the multi-strain time series are known, the number of susceptibles at time t for strain i:

$$S_{t,i} = S_{t-1,i} + B_t - I_{t,i} - \delta \left[\sum_{j \neq i} I_{t,j} - \frac{1}{1-e^{-L/\lambda}} \sum_{j \neq i} \sum_{t'=t-L}^{t-1} I_{t',j} e^{-(t-t')/\lambda} (e^{1/\lambda} - 1) \right] \quad (7)$$

This formulation removes individuals infected with any serotype at time t from the susceptible pool of individuals of strain i. Those infected with serotype i never return to the susceptible class for serotype i, but those infected with one of the other j serotypes trickle back into the susceptible pool for serotype i. We define

$$Q_{t,j} = \sum_{w=1}^{t} \hat{\rho}_{w,j} C_{w,j} - \sum_{w=1}^{t} \sum_{v=0}^{L-1} \hat{\rho}_{w-v,j} C_{w-v,j} Pr_\lambda(v < X < v+1 | X < L)$$

for all $t > L$.

2 Testing the robustness of the model: simulation studies

2.1 Data generation

We tested our methods on simulated data from a system developed independently by a subset of co-authors [Shrestha et al., 2011]. We analyzed 12,000 simulated data sets from their continuous-time multi-strain state-space model that incorporates cross-protection (as partial protection in individuals that decays exponentially over time) and susceptible enhancement.

We generated simulated datasets by varying three parameters: the reporting fraction (either 10% or 1%), the average duration of cross-protection (1 day, 6 months, 1 year, 1.5 years, 2 years or 3 years) and the inclusion of susceptible enhancement (included as either a 40% increased risk of secondary infection or no increased risk). For each of the 24 possible combinations of parameters, 500 datasets

were simulated, for a total of 12,000 datasets. Neither seasonal nor serotype-specific variability in transmission rates were included in the data generating model. For a complete list of parameters used to generate the simulated data, see Supplementary Table 3.

2.2 Analyzing simulated datasets

Each of the 12,000 simulated datasets was analyzed assuming an exponential distribution of the duration of cross-protection. We assumed that reporting rates remained constant but were different for each serotype. In generating the data, the reporting rate remained constant over the entire time period and was the same for each serotype. Models N, N_a, N_b, N_c, N_d, E_a, E_b, E_c, and E_d (as specified in Supplemental Table 1) were all fit to each dataset and the log-likelihood of each model was stored. For each dataset, the one of the nine models with the lowest AIC was chosen as the "best" model.

Supplemental Figure 3 shows the average estimated durations of cross-protection from the chosen best models. Overall, the estimated duration of cross-protection from the TSIR model (shown in blue) appeared to, on average, very nearly unbiased although often marginally lower than the true average duration of cross-protection (shown in red).

Supplemental Figure 4 shows the empirical 95% confidence interval coverage for λ, the average duration of cross-protection. The coverage rates appear to depend on both the true duration of cross-protection and the fraction of cases reported. When no cross-protection is present, the coverage is above 90% for datasets with 10% of cases reported. These coverage rates decline as the duration of cross-protection increases. In general, it appears that enhancement does not have a large impact on the coverage rates.

The reporting rates were on average underestimated by 25%. This underestimation was consistent across all 24 combinations of parameters, suggesting that a difference between the data generation model and the assumed statistical model may account for this systematic bias. For example, the data generation model assumes that each individual achieves permanent immunity to all serotypes after two infections. The estimation framework assumes that each individual in infected by all four serotypes exactly once. The observed underestimation of reporting rates could be due to the difference in these model assumptions.

2.3 Simulating data from the TSIR model

To investigate whether our estimated models could generate multi-annual patterns displayed in the observed incidence data we simulated serotype-specific incidence over the time-period of the observed data. Using Fourier transforms, we estimated the frequency of multi-annual oscillations in the simulated data and compared this to empirical data.

We have 38 years of observed data and, as descried in the Materials and Methods section of the main paper, we used the first 10 years and 5 months to define the initial state of the system. Then we simulated the remaining observations, using the observed birth data, fitted model parameters and the

initial estimated $Z_{t,i}$. Because $Z_{t,i} = \bar{S} + S_{t,i}$, we can rewrite equation 6 as

$$Z_{t,i} = Z_{t-1,i} + B_{t-d} - I_{t,i} - \delta \sum_{j \neq i} [I_{t-1,j} - I_{t-(k+1),j}]. \quad (8)$$

Therefore, using equation 5 and the equation above, we iterated back and forth to simulate new serotype-specific incidence data. To compare the impact that cross-protection has on the multi-annual dynamics of the overall system, we simulated 1000 datasets from our best-fitting fixed duration cross-protection model, F_c, and 1000 datasets from our best-fitting model that did not include cross-protection, N_c. The data were necessarily simulated on the scale of the fully-observed and unreported data (i.e. on the scale of I_t and not of C_t). However, before any computation was performed on the simulated datasets, the data were re-scaled to be on the scale of the observed case counts. The sampling was taken as binomial draws from the simulated case counts with an observation probability based on the estimated $\hat{\rho}_{t,i}$, which change over time. The resulting simulated datasets are shown in Supplemental Figure 1. For each simulated dataset, we computed and plotted the Fourier spectrum and also computed the cycle length with the highest Fourier coefficient (see Supplemental Figure 2). Before calculating the spectra, the simulated data were detrended and normalized.

In Supplemental Figure 2, we show the serotype-specific spectra for the observed data as well as for the simulated datasets. The histograms on the bottom show the distribution of strongest observed cycle-length (across all serotypes). In the models with no cross-protection (in red, on the left), we see evidence of strong annual cycles. Apart from these annual cycles, the strongest cycle lengths appear to be fairly uniformly distributed across the rest of the durations, especially between 4 and 15 years. In the simulated datasets from a system that includes an average cross-protection of 2 years (as in model F_c), we again see strong annual cycles. In addition, there is evidence of more consistent 3 to 5 year cycles in the simulated data when cross-protection is included.

The TSIR framework, therefore, appears to fit models that generate data consistent with the observed shorter multi-annual cycles. However the longer cycles in the observed data (on the order of 8-15 years) are not captured in these simulations. These cycles do possibly represent actual periodicities of the disease system, but they may also be influenced by the long-term artifacts of the surveillance system, such as changing reporting rates.

References

Benjamin M Bolker. *Ecological Models and Data in R*. Princeton University Press, August 2011.

Matthew J Ferrari, Rebecca F Grais, Nita Bharti, Andrew J K Conlan, Ottar N Bjørnstad, Lara J Wolfson, Philippe J Guerin, Ali Djibo, and Bryan T Grenfell. The dynamics of measles in sub-Saharan Africa. *Nature*, 451(7179):679–684, February 2008.

BF Finkenstädt and Bryan T Grenfell. Dynamics of measles epidemics: estimating scaling of transmission rates using a time series SIR model. *Ecological . . .*, 2002.

BF Finkenstädt and BT Grenfell. Time series modelling of childhood diseases: a dynamical systems approach. *Journal of the Royal Statistical Society Series C-Applied Statistics*, 49:187–205, 2000.

K Glass, Y Xia, and BT Grenfell. Interpreting time-series analyses for continuous-time biological models—measles as a case study. *Journal of theoretical biology*, 223(1):19–25, 2003.

Wei-min Liu, Herbert W Hethcote, and Simon A Levin. Dynamical behavior of epidemiological models with nonlinear incidence rates. *Journal of mathematical biology*, 25(4):359–380, 1987.

C Jessica E Metcalf, Ottar N Bjørnstad, Bryan T Grenfell, and Viggo Andreasen. Seasonality and comparative dynamics of six childhood infections in pre-vaccination Copenhagen. *Proceedings of the Royal Society B: Biological Sciences*, 276(1676):4111–4118, December 2009.

Ananda Nisalak, Timothy P Endy, Suchitra Nimmannitya, Siripen Kalayanarooj, Usa Thisayakorn, Robert M Scott, Donald S Burke, Charles H Hoke, Bruce L Innis, and David W Vaughn. Serotype-specific dengue virus circulation and dengue disease in Bangkok, Thailand from 1973 to 1999. *American Journal of Tropical Medicine and Hygiene*, 68(2):191–202, February 2003.

Sourya Shrestha, Aaron A King, and Pejman Rohani. Statistical inference for multi-pathogen systems. *PLoS computational biology*, 7(8):e1002135, August 2011.

Table 1: **Parameter estimates from models and metrics for model performance.** Each row represents a fitted model with a different set of assumptions. Results from models that assumed no cross protection (N), a fixed duration of cross protection ("f. d.", F) or exponential cross protection ("exp", E) are presented. A large dot in the R, S and T columns indicate inclusion of serotype- and time-varying reporting fractions (R), serotype-specific transmission rates (S), and time-varying transmission rates (T). The degrees of freedom (DF) for each model can be found is also displayed. The final column (cor) shows the correlations between observed data and predictions from the model.

CP	M	R	S	T	lambda	alpha1	loglik	DF	cor	BIC	AIC	AICc
none	N	-	-	-	-	$_{0.895}\,0.912\,_{0.929}$	-902.4	3	0.832	1827.9	1810.9	1810.9
	N_a	•	-	-	-	$_{0.997}\,0.999\,_{1.001}$	-946.7	15	0.952	2008.5	1923.5	1923.7
	N_b	•	•	-	-	$_{0.864}\,0.884\,_{0.903}$	-882.9	19	0.951	1911.6	1803.8	1804.2
	N_c	•	-	•	-	$_{0.869}\,0.888\,_{0.908}$	-817.2	41	0.955	1949.0	1716.5	1718.1
	N_d	•	•	•	-	$_{0.865}\,0.885\,_{0.905}$	-781.1	119	0.953	2475.0	1800.1	1814.2
f. d.	F_a	•	-	-	$_{0.16}\,0.48\,_{1.57}$	$_{0.997}\,0.999\,_{1.001}$	-941.8	17	0.953	2013.9	1917.5	1917.8
	F_b	•	•	-	$_{0.99}\,2.13\,_{2.72}$	$_{0.850}\,0.870\,_{0.890}$	-870.5	21	0.953	1902.0	1782.9	1783.3
	F_c	•	-	•	$_{0.75}\,2.00\,_{3.10}$	$_{0.856}\,0.876\,_{0.896}$	-807.3	43	0.958	1944.5	1700.7	1702.5
	F_d	•	•	•	$_{0.75}\,1.93\,_{3.18}$	$_{0.852}\,0.873\,_{0.893}$	-771.0	121	0.955	2470.2	1784.0	1798.6
exp.	E_a	•	-	-	$_{0.19}\,0.77\,_{5.65}$	$_{0.997}\,0.999\,_{1.001}$	-943.3	16	0.953	2009.3	1918.6	1918.8
	E_b	•	•	-	$_{1.00}\,2.23\,_{6.65}$	$_{0.856}\,0.876\,_{0.896}$	-873.9	20	0.953	1901.2	1787.8	1788.2
	E_c	•	-	•	$_{0.88}\,1.88\,_{4.31}$	$_{0.862}\,0.882\,_{0.901}$	-810.0	42	0.957	1942.2	1704.0	1705.7
	E_d	•	•	•	$_{1.00}\,2.27\,_{6.85}$	$_{0.858}\,0.878\,_{0.898}$	-773.5	120	0.954	2467.5	1787.0	1801.3

Table 2: **Model estimated number of reported cases per 1000 incident cases.** Shown are the minimum, median, and maximum reporting rates by model (E_c and F_c) and serotype.

Model	serotype	minimum	median	maximum
F_c	1	1.05	1.20	2.54
	2	0.85	0.99	1.27
	3	0.79	1.00	1.58
	4	0.31	0.38	0.78
E_c	1	1.03	1.18	2.61
	2	0.83	0.97	1.25
	3	0.78	0.99	1.51
	4	0.31	0.37	0.71

Table 3: Parameters used to independently generate datasets from which we estimated the duration and strength of cross-protection. When applicable, the notation from [Shrestha et al., 2011] is provided. The top three parameters were varied across datasets.

simulation parameter	assumed value(s)	estimated
duration of cross-protection, $\frac{1}{\Delta}$	1 day, 6, 12, 18, 24, 36 months	Yes
reporting rates	1% and 10%	Yes
enhancement, χ	1 and 1.4	No
population size, N	10 million	No
per capita birth rate, μ	0.02 per year	No
per capita death rate, μ	0.02 per year	No
transmission rate, β	70 per year	No
rate of recovery, γ	26 per year	No
force of infection due to immigration, ω	5 x $10^{-}7$	No
Std. deviation of white noise $\frac{\partial W}{\partial t}$, η	0.005	

Figure 1: The observed serotype-specific case counts (red line) compared to 1000 simulated datasets (transparent blue lines). These data were simulated from model F_c. For each serotype, one sample simulated trajectory is shown in black.

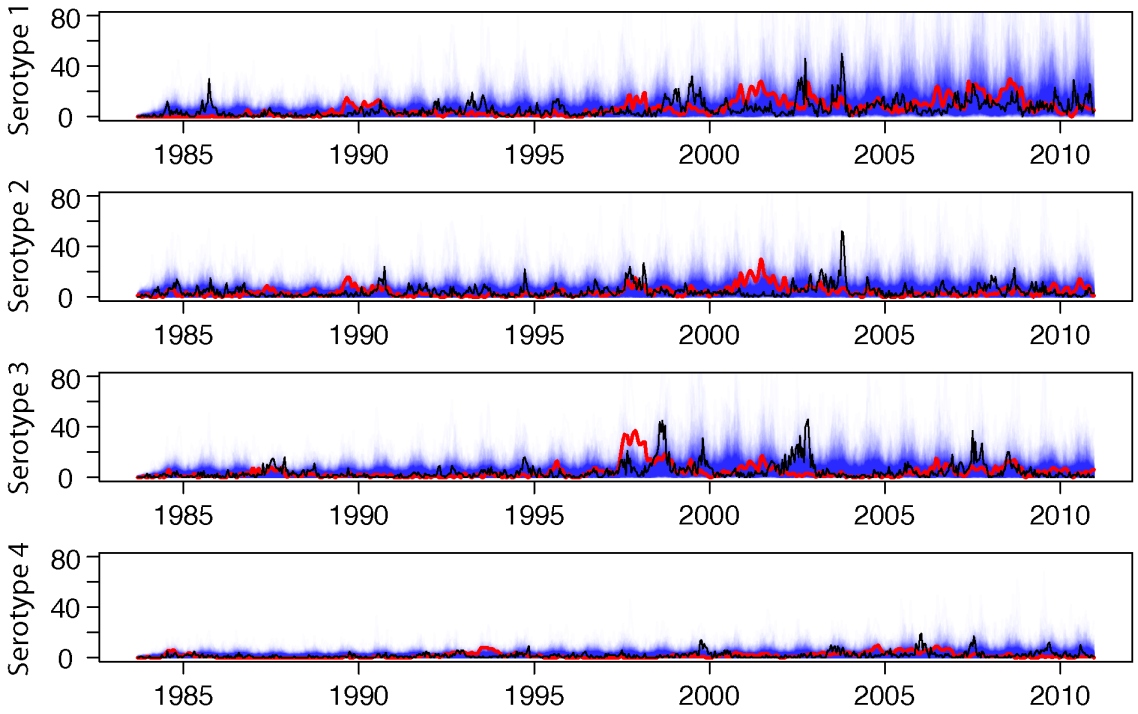

Figure 2: Comparing Fourier spectra of simulated and real data. The left-hand (red) column shows spectra from 1000 datasets simulated in systems with no cross-protection. The right-hand (blue) column shows spectra from 1000 datasets assuming an average two-year cross-protection (from model F_c). The black lines represent the spectra of the observed serotype-specific data. The histograms on the bottom show the distribution of strongest observed cycle-length for each of the 1000 datasets.

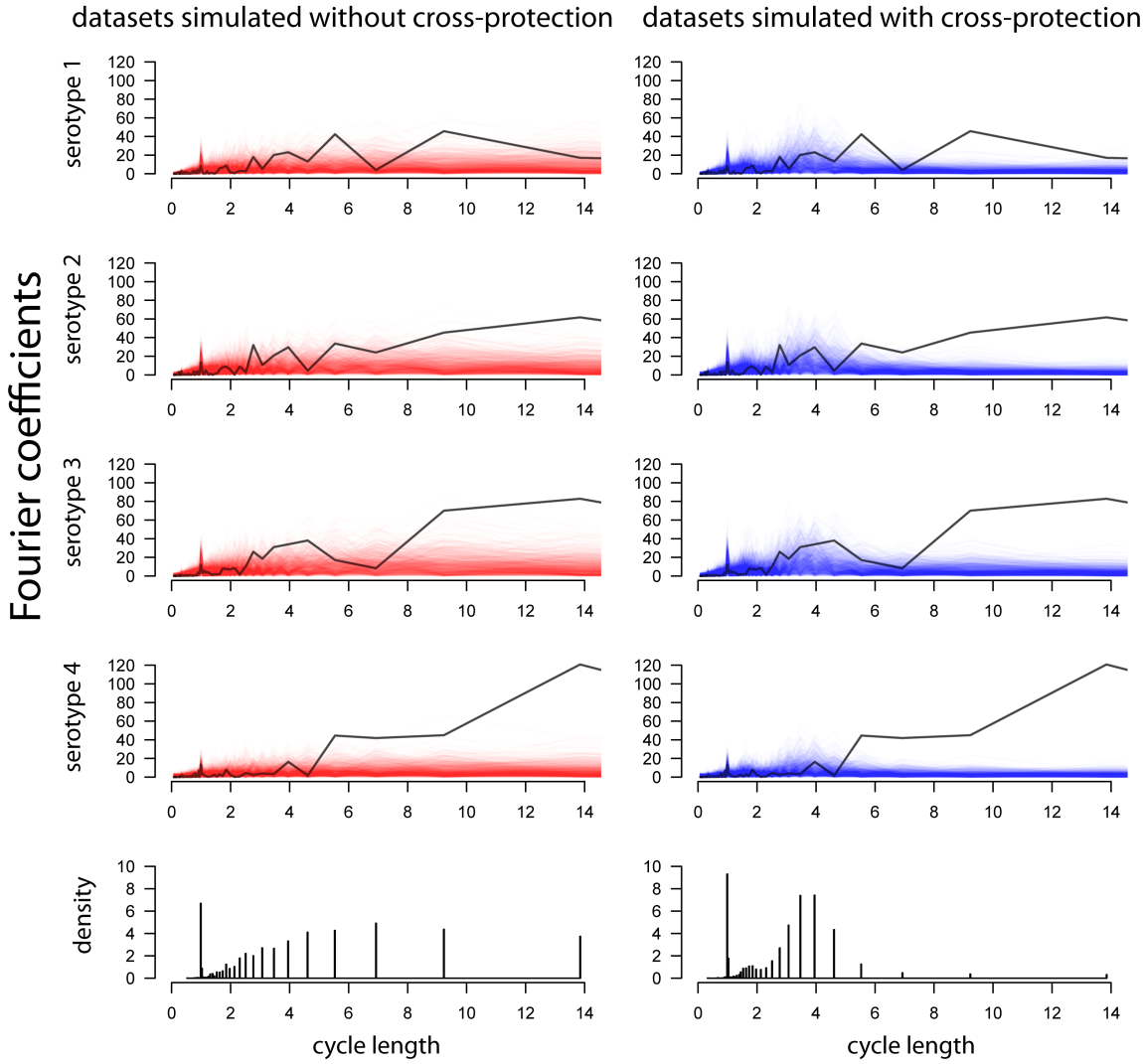

Figure 3: Comparing estimated durations versus the truth. This figure shows the average estimated durations of cross-protection from the best model for each dataset, based on AIC. The mean estimated average duration of cross-protection from the TSIR models in each simulation scenario is denoted by a vertical blue line. The true average duration of cross-protection is given by a vertical red line. The four rows of boxes represent the factorial simulation design across scenarios with susceptibility enhancement (E) or not (no E) and reporting rates (10% and 1%). The columns of boxes sweep across the six different average durations of cross-protection used in the simulation study.

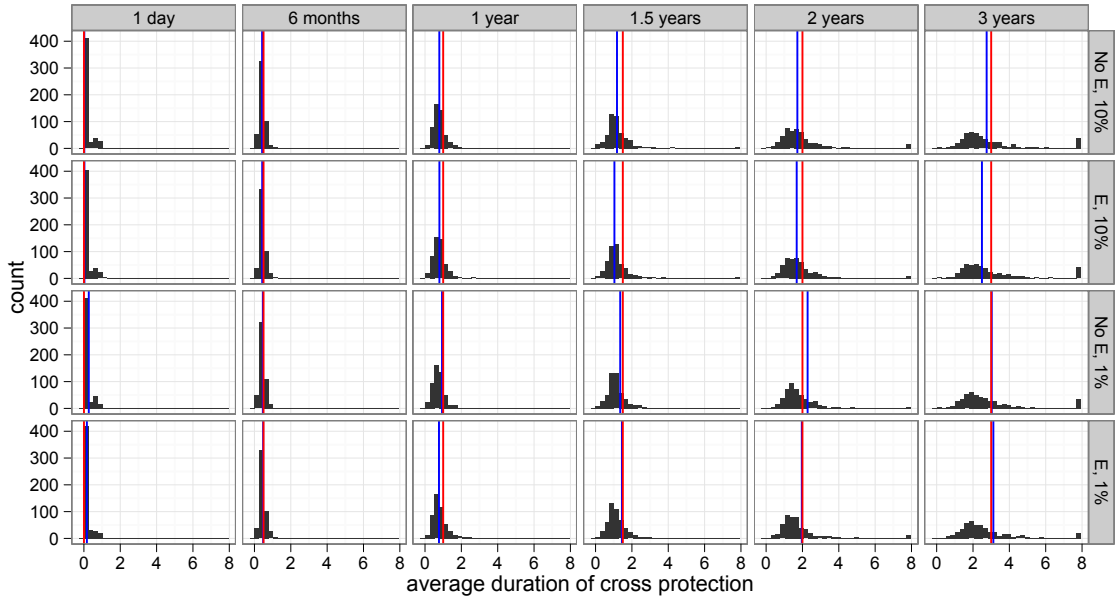

Figure 4: TSIR model estimation performance metrics. This figure shows the empirical 95% confidence interval coverage for λ, the average duration of cross-protection. The color of the lines encodes whether enhancement was present (orange) or not(blue) in the system that generated the simulated data. Dashed lines correspond to datasets with 1% reporting rates and solid lines are for datasets with 10% case reporting rates.

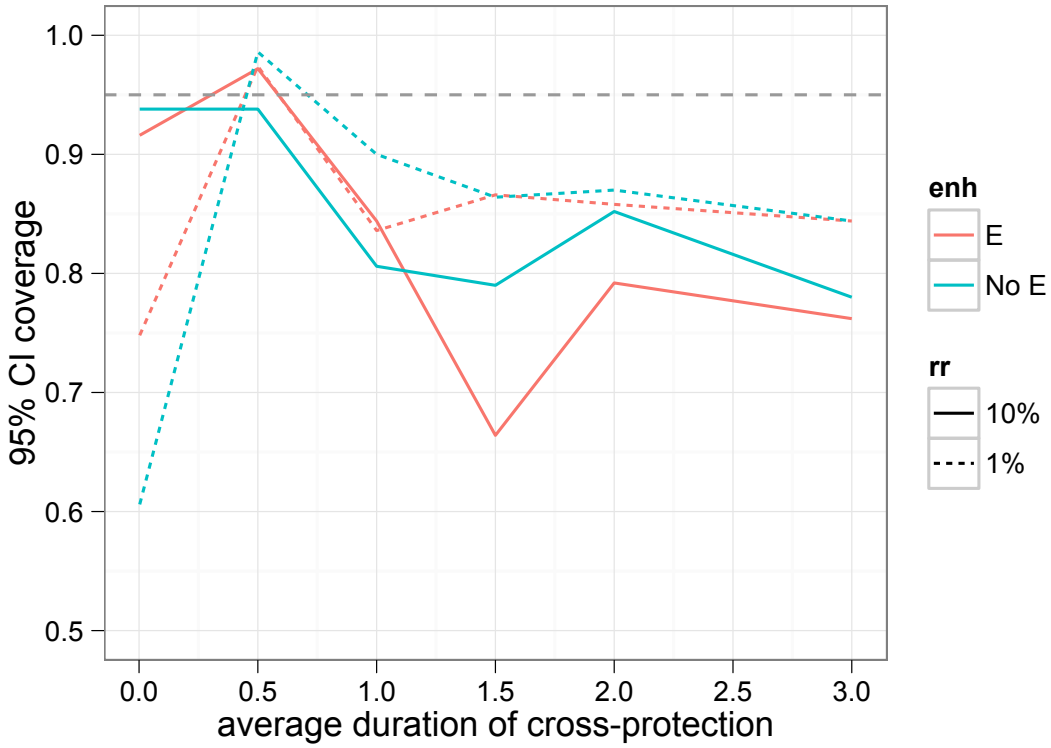

Figure 5: The full likelihood profile from model F_c. This figure shows the likelihood profile for values of δ between -1 and 1. The two lightest shades of blue indicate the 90th and 95th bivariate confidence regions. The regions with no color indicate places where the susceptible accounting iterative algorithm failed to converge.

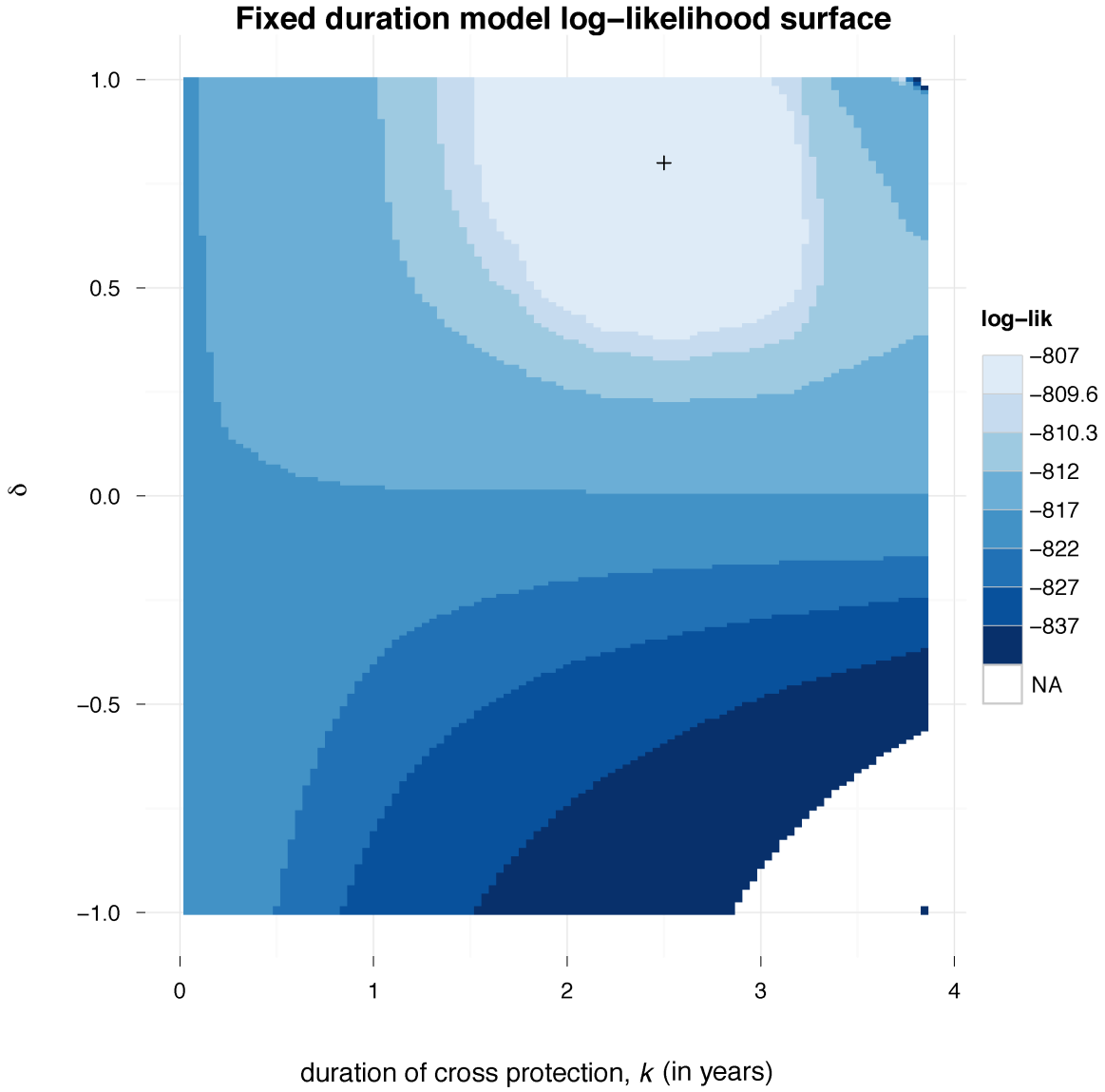

Figure 6: Compartment model representation. Compartment CP is the "convalescent" or "cross-protected" group, which depends on the number of infecteds from other serotypes. The S, I and R compartments are the standard susceptible, infected and recovered classes.